

Jarred R. Mondoñedo

Department of Biomedical Engineering,
School of Medicine,
Boston University,
Boston, MA 02215

John S. McNeil

Department of Anesthesiology,
University of Virginia,
Charlottesville, VA 22903

Jacob Herrmann

Department of Anesthesiology;
Department of Biomedical Engineering,
University of Iowa,
Iowa City, IA 52242

Brett A. Simon

Department of Anesthesiology
and Critical Care Medicine;
Department of Surgery,
Memorial Sloan Kettering Cancer Center,
New York, NY 10065

David W. Kaczka¹

Department of Anesthesiology, Biomedical
Engineering, and Radiology;
Department of Biomedical Engineering;
Department of Radiology,
University of Iowa Hospitals and Clinics,
Iowa City, IA 52242
e-mail: david-kaczka@uiowa.edu

Targeted Versus Continuous Delivery of Volatile Anesthetics During Cholinergic Bronchoconstriction

Volatile anesthetics have been shown to reduce lung resistance through dilation of constricted airways. In this study, we hypothesized that diffusion of inhaled anesthetics from airway lumen to smooth muscle would yield significant bronchodilation in vivo, and systemic recirculation would not be necessary to reduce lung resistance (R_L) and elastance (E_L) during sustained bronchoconstriction. To test this hypothesis, we designed a delivery system for precise timing of inhaled volatile anesthetics during the course of a positive pressure breath. We compared changes in R_L , E_L , and anatomic dead space (V_D) in canines ($N=5$) during pharmacologically induced bronchoconstriction with intravenous methacholine, and following treatments with: (1) targeted anesthetic delivery to V_D and (2) continuous anesthetic delivery throughout inspiration. Both sevoflurane and isoflurane were used during each delivery regimen. Compared to continuous delivery, targeted delivery resulted in significantly lower doses of delivered anesthetic and decreased end-expiratory concentrations. However, we did not detect significant reductions in R_L or E_L for either anesthetic delivery regimen. This lack of response may have resulted from an insufficient dose of the anesthetic to cause bronchodilation, or from the preferential distribution of air flow with inhaled anesthetic delivery to less constricted, unobstructed regions of the lung, thereby enhancing airway heterogeneity and increasing apparent R_L and E_L . [DOI: 10.1115/1.4040001]

1 Introduction

Acute exacerbations of bronchoconstriction may be severe, life-threatening, and refractory to conventional bronchodilator therapy. Treatments for severe bronchoconstriction may involve inhaled β_2 -agonists or helium-oxygen mixtures, short-term infusions of magnesium sulfate, or more invasive techniques such as extracorporeal membrane oxygenation [1,2]. A clinically relevant alternative treatment strategy is the use of inhaled volatile anesthetic agents such as halothane, isoflurane, sevoflurane, or desflurane, since all are potent bronchodilators [3–7]. As described in multiple case reports and small series [8–12], treatment with volatile anesthetics generally results in improvement within 12 h. However, these agents have been used for periods of several days in refractory cases. Volatile anesthetics have also been shown to be effective in pediatric and obstetric patients [5–7,13–15]. Reduced hospital length of stay and duration of mechanical ventilation have also been observed in patients treated with inhaled isoflurane [16].

Despite their therapeutic potential, routine clinical use of inhaled anesthetic agents may be limited by predictable hemodynamic and sedative side effects [1], especially in patients without a secured

airway. Other negative side effects, such as myocardial and respiratory depression, arrhythmias, intrapulmonary shunting, muscle relaxation, and cerebral vasodilation may require supplemental pharmacological interventions that may limit the administered dose [17]. Hepatic and renal dysfunction can also be a risk during more prolonged cases [16]. Thus, there are few data available regarding the optimal administration of these agents [3,18].

The dominant mechanism of bronchodilation for these agents is not completely understood [19]. Volatile anesthetics induce direct relaxation of airway smooth muscle (ASM) by the reduction of intracellular free calcium via inhibition of protein kinase C, calcium release from sarcoplasmic reticulum, or voltage-dependent calcium channels [20–22]. In addition, volatile anesthetics are known to reduce the sensitivity of the myofibrillar contractile apparatus to intracellular calcium [23]. In vivo, bronchodilation with inhaled agents depends on diffusion across the airway wall to reach their pharmacologic site of action [24,25]. While this may be most readily achieved via luminal diffusion across the airway wall, systemic uptake and distribution to ASM is also possible via the bronchial or pulmonary circulations. Inhaled anesthetic agents also dilate airways indirectly by reducing vagal tone and reflexes, and by altering β -receptor sensitivity and circulating catecholamines [26–28].

We recently proposed that direct action of inhaled anesthetic agents on ASM would be an effective mechanism for bronchodilation in vivo, and that targeted delivery of these agents to the

¹Corresponding author.

Manuscript received January 24, 2018; final manuscript received April 13, 2018; published online May 9, 2018. Assoc. Editor: Geoffrey Maksym.

conducting airways would promote ASM relaxation with a reduction in systemic absorption [29]. In this study, we hypothesized that diffusion of inhaled anesthetics from airway lumen to ASM would yield significant bronchodilation in vivo, and systemic recirculation would not be necessary to reduce lung resistance and elastance during sustained bronchoconstriction. To test this hypothesis, we developed a novel anesthetic-ventilator system to deliver volatile agents selectively to the conducting airways, or continuously to both the conducting airways and gas exchanging alveolar region. To compare these approaches, we measured lung mechanics and anatomic dead space during sustained cholinergic bronchoconstriction in dogs, before and after continuous and targeted anesthetic delivery.

2 Methods

2.1 Anesthetic Delivery System. To achieve targeted delivery of the volatile anesthetic to the conducting airways of the lung, we designed and implemented a unique ventilator-valve circuit for precise control of timing and duration of inhaled agent. The inspiratory limb of a transport ventilator (Impact Instrumentation, Inc., West Caldwell, NJ) was divided into two sublimbs (Fig. 1). Flow through each sublimb was regulated using computer-actuated solenoid-valves (ASCO Valve, Florham Park, NJ). For targeted delivery, inspiratory flow was initially directed through the bypass sublimb. Following actuation of the solenoid valves, the inspiratory flow was then directed through the second sublimb containing a Universal Portable Anesthesia Complete (U-PAC) drawover vaporizer (Datex-Ohmeda, GE Healthcare, Fairfield, CT). Both sublimbs were rejoined into a single inspiratory limb that was connected to the airway opening.

Precise switching between sublimbs was accomplished using custom-written data acquisition and control software (National Instruments LabVIEW 2011, Austin, TX). The software estimated the tidal volume (V_T) on a breath-by-breath basis, using trapezoidal integration of the measured flow signal (\dot{V}) [30]. For volumes below a user-defined threshold volume (V_{th}), fresh gas was directed through the bypass sublimb. When the delivered volume exceeded V_{th} , the software actuated a relay driver circuit via a D/A board. The actuating signal inverted the open/closed configuration of the solenoid valves, forcing the inspiratory gas through the vaporizer sublimb and delivering a bolus of anesthetic agent (with known concentration) in the subsequent portion of V_T through the end of inspiration. Changing the minimum volume V_{th} for which the vaporizer was engaged during inspiration, allowed us to vary the timing and duration of anesthetic delivery.

One-way check valves (Hans Rudolph, Inc., Series 1240C, Shawnee, KS) were included in the circuit to ensure a unidirectional flow within the inspiratory limb and to prevent backflow during the expiratory phase. Passive expiration occurred via a bidirectional mushroom valve. Expired gas was directed into an active scavenging system. Precise delivery of the inhaled anesthetic relies on accurate estimates of V_T , which may be influenced by slow drifts, transient fluctuations, gas removal by the side-stream gas analyzer, and other minor fluxes. To minimize these inaccuracies, the numerical integrator was reset to zero at the onset of each new breath, such that V_T was independent of the previous breath and any minor fluctuations. Individual breaths were identified using a numerical breath detector designed to distinguish transitions between inspiration and expiration based on the measured \dot{V} .

2.2 In Vitro Validation. Proof-of-concept experiments were conducted with the anesthetic ventilator system to quantify inhaled anesthetic delivery to a given dead space volume (V_D). The apparatus consisted of a length of 22 mm ID corrugated tubing with a total volume of about 150 ml, in series with two spring-loaded bellows (IngMar Medical, Ltd. Adult/Pediatric Demonstration Lung, Pittsburgh, PA). This mechanical model simulated a conducting airway or “dead space” compartment, in series with an “alveolar” compartment. During ventilation of the test lung, anesthetic concentrations were measured at the front end (“airway opening”), midpoint, and

terminal end (“alveolar/airway mixing interface”) of the tubing segment, using a side-stream infrared gas analyzer (Datex-Ohmeda Capnomac Ultima, GE Healthcare).

2.3 Animal Preparation and Measurements. Animal experiments were conducted in the Animal Research Facility at Beth Israel Deaconess Medical Center, with Protocol #048-2012 approved by the Institutional Animal Care and Use Committee. Measurements were obtained in five mongrel male dogs weighing between 20 and 25 kg. General anesthesia was induced and maintained with intravenous midazolam (induction dose 10–20 mg, maintenance infusion $0.25 \text{ mg kg}^{-1} \text{ h}^{-1}$) and fentanyl (induction dose 200–250 μg , maintenance infusion $2\text{--}5 \mu\text{g kg}^{-1} \text{ h}^{-1}$). Each animal was intubated with an endotracheal tube (8.0 mm ID). Neuromuscular blockade was achieved with 1–2 mg intravenous boluses of vecuronium every 10–15 min. Electrocardiogram, oxygen saturation, heart rate were monitored continuously, and noninvasive blood pressure was cycled every 3–5 min. Each animal was ventilated at an initial rate of 20 min^{-1} , V_T of 15 ml kg^{-1} , and positive end-expiratory pressure (PEEP) of $0 \text{ cmH}_2\text{O}$ PEEP. The rate and V_T were titrated to achieve end-tidal CO_2 pressures between 20 and 40 mmHg. To ensure sufficient oxygenation during bronchoconstriction, animals were ventilated with 100% O_2 throughout the experiment.

Pressure (P_{ao}) and flow (\dot{V}) at the airway opening were measured using a pneumotachograph system (Hans Rudolph RSS100-HR, Kansas City, MO), which was appropriately corrected for ventilation with 100% O_2 . An esophageal balloon catheter (Ackrad Labs, Cooper Surgical, Trumbull, CT) was placed in the lower third of the esophagus to measure esophageal pressure (P_{es}), which served as a surrogate for pleural pressure. Transpulmonary pressure (P_{tp}) was estimated as the difference between P_{ao} and P_{es} . The P_{ao} , P_{es} , and \dot{V} signals were low-pass filtered at 10 Hz (Frequency Devices, Inc., 90IP, Ottawa, IL), and sampled at 40 Hz using a 12-bit analog-to-digital converter (National Instruments NI UB-6008, Austin, TX). Anesthetic, O_2 , and CO_2 concentrations were measured at the airway opening using a side-stream infrared gas analyzer (Datex-Ohmeda Capnomac Ultima, GE Healthcare), and digitized using the same A/D board. All sampled waveforms were stored on a laptop computer (Acer Aspire 5733Z, San Jose, CA).

2.4 Experiment Protocol. To compare the bronchodilatory efficacy of different inhaled anesthetic delivery regimens and agents, all animals were subjected to four separate experiments applying either targeted or continuous delivery of sevoflurane or isoflurane. Each animal served as its own control. The experimental protocols were applied in random order, with each experiment performed at least one week apart. A description of the experimental protocol is shown in Fig. 2. Following intravenous anesthetic induction, baseline measurements of P_{ao} , P_{es} , and \dot{V} waveforms were sampled for 20 breaths. Prior to each measurement of R_L , E_L , and V_D , two deep inspirations were performed to standardize volume history. Sustained bronchoconstriction was then induced with intravenous infusion of methacholine (MCh) at $100 \mu\text{g min}^{-1}$. A separate intravenous line was used for the MCh infusion, in order to minimize transient effects of the periodic neuromuscular blockade boluses. All pressure and flow measurements were obtained after establishing a sufficient level of steady-state bronchoconstriction [31].

Following bronchoconstriction with MCh, either targeted or continuous inhaled anesthetic delivery was initiated and maintained for a total of 20 min. Pressure and flow waveforms were recorded at 10 and 20 min during this period. Inhaled anesthetic concentration was manually adjusted on the U-PAC vaporizer, to attain peak values of 1–2 minimum alveolar concentration (MAC) for dogs [32]. During continuous delivery, intravenous midazolam and fentanyl infusion rates were decreased based on blood pressure, to maintain appropriate anesthetic depth. The MCh infusion was suspended at the conclusion of the experiment, and each animal was administered a 4 mg intravenous of atropine for maximal bronchodilation. Reversal of neuromuscular blockade was achieved

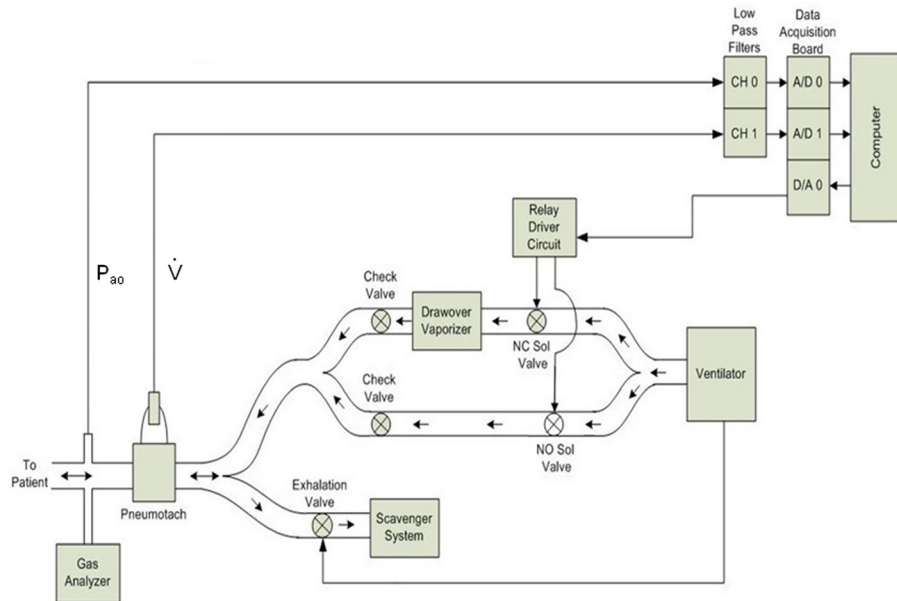


Fig. 1 Schematic of inhaled anesthetic delivery system. Arrows within the ventilator circuit denote direction of flows. NO Sol, normally open solenoid valve; NC Sol, normally closed solenoid valve; A/D, analog-to-digital converter; D/A, digital-to-analog converter; P_{ao} , airway pressure; \dot{V} , airway flow. Check valves included to prevent back flow into the inspiratory limb as the gas travels to the scavenger system during expiration.

with intravenous boluses of glycopyrrolate (0.2 mg) and neostigmine (1.5 mg). After final measurements of P_{ao} , P_{es} , and \dot{V} , each animal emerged from general anesthesia and was extubated. In order to ensure animal safety and anesthetic depth, as well as deliver appropriate inhaled anesthetic during either targeted or continuous delivery, the investigators were not blinded to condition.

2.5 Data Analysis. The sampled P_{tp} , V , and \dot{V} waveforms were fitted to a single-compartment model using multiple linear regression [30]

$$P_{tp} = R_L \dot{V} + E_L V + P_0$$

where R_L and E_L are lung resistance and elastance, respectively, and P_0 is the transpulmonary pressure at end-expiration. Prior to

each regression, airway pressure measurements were corrected for nonlinear effects of the endotracheal tube [33].

Changes in V_D were estimated for each breath using the technique of volume capnography [34]. Briefly, a volume capnogram for each breath was divided into three phases (Fig. 3) corresponding to: (I) resident gas in the conducting airways at the end of inspiration; (II) gas mixing at the interface between terminal bronchi and alveoli; and (III) gas expired primarily from the alveoli. A vertical line parallel to the y-axis of the capnogram was placed through phase II, such that the area to the left of the vertical line and below the curve was equal to the area to the right of the vertical line and between the curve and a line tangent to the linear portion of phase III. Total V_T was then divided into an anatomic dead

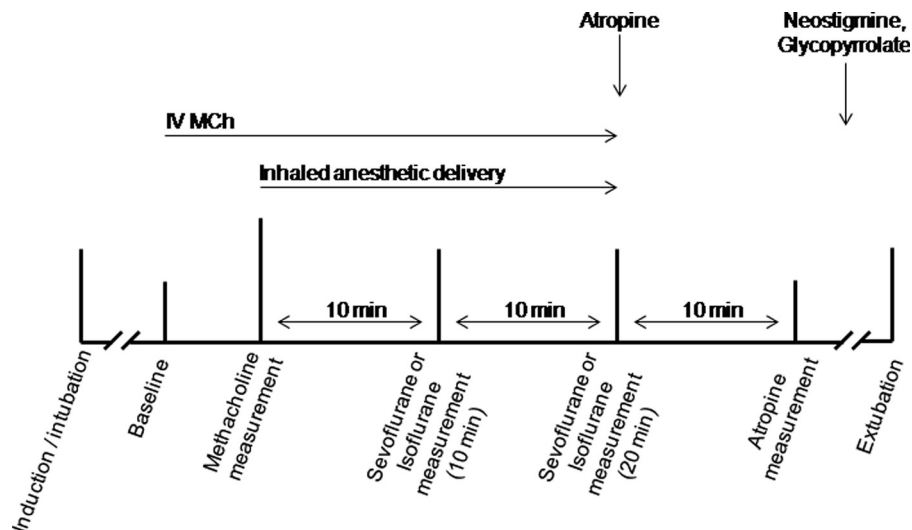


Fig. 2 Timeline of experimental protocol and drug administration. Baseline measurements of R_L , E_L , and V_D were obtained after anesthetic induction and intubation. Intravenous MCh was then used to induce sustained bronchoconstriction, followed by either targeted or continuous delivery of the inhaled anesthetic. Intravenous atropine was administered after treatment with inhaled anesthetic. Neostigmine and glycopyrrolate were used at the end of the protocol, to reverse neuromuscular blockade.

space volume (V_D) and an effective “alveolar” tidal volume (V_{alv}). From the capnogram, the volumes along the x -axis to the left and right of the vertical line were assumed to correspond to V_D and V_{alv} , respectively.

To compare the quantities of inhaled anesthetic each animal received during the targeted or continuous delivery regimens, the anesthetic dose was monitored on a breath-by-breath basis by plotting the concentration of anesthetic agent (C_{agent}) as a function of V_T . The volume of anesthetic agent inhaled during each breath (V_{agent}) was estimated by numerical integration of the inspiratory portion of the resulting curve.

2.6 Statistics. One-way repeated measures analysis of variance (ANOVA) was used to compare estimates of R_L , E_L , and V_D for targeted and continuous delivery of both sevoflurane and isoflurane. Two-way repeated measures ANOVA was used to compare the inhaled anesthetic dose per breath, with factors selected to be (1) targeted or continuous delivery, and (2) the time point of measurement. If significance was obtained with ANOVA, post hoc analysis was performed using the Holm–Sidak criterion. For each measurement condition, comparisons of R_L , E_L , and V_D were made for targeted and continuous delivery using two-tailed paired t -tests. For all comparisons, $P < 0.05$ was considered statistically significant. Sample size necessary to detect significant changes in R_L during MCh infusion was estimated based on our previous experience with pharmacologically induced bronchoconstriction in dogs [31,35]. All model fits, parameter estimations, and statistical analyses were performed using either MATLAB R2012a (The Mathworks, Inc., Natick, MA) or SigmaPlot 12.3 (Systat Software, Inc., San Jose, CA).

3 Results

3.1 In Vitro Validation. Characteristic traces of \dot{V} , V_T , and isoflurane concentrations during targeted delivery to a length of corrugated tubing in series with spring-loaded bellows is shown in Fig. 4. Isoflurane was not detectable at the interface between the medical tubing and the spring-loaded bellows, indicating that the anesthetic was constrained to the simulated dead space volume. We also found that the concentration of isoflurane within the

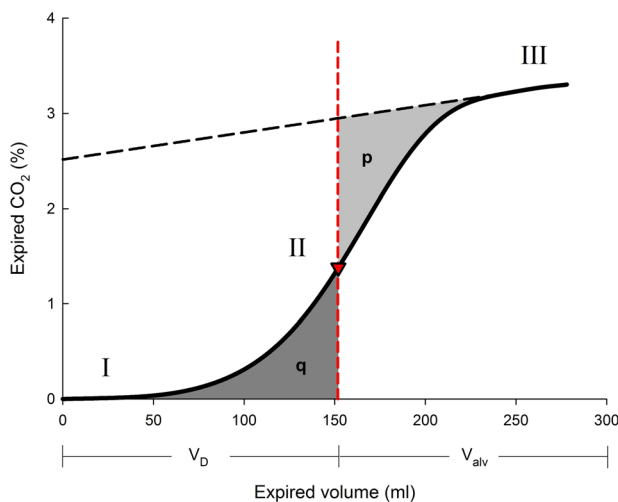


Fig. 3 Real-time estimation of anatomic dead space using the technique of volume capnography in a representative dog; this analysis was automated for each breath as part of the solenoid-valve control software. A line tangent to phase III (sloping upward dashed) and a vertical line through phase II (vertical dashed) are positioned such that areas p and q are equal. Volumes along the x -axis to the left and right of the vertical line are assumed to correspond to the dead space volume (V_D), and the effective alveolar volume (V_{alv}), respectively.

tubing decreased longitudinally, from the airway opening to the “alveolar” compartment. Moreover, we importantly observed that the concentration of isoflurane at end-expiration was negligible for each sampling location, indicating that the majority of the delivered anesthetic was removed after each breath.

3.2 Targeted Versus Continuous Delivery. Figure 5 summarizes R_L , E_L , and V_D for all five dogs under baseline conditions, after maximal bronchoconstriction with MCh, at 10 and 20 min of inhaled anesthetic delivery, and following reversal of bronchoconstriction with atropine. Compared to baseline, we found that MCh significantly increased R_L and E_L , and decreased V_D prior to delivery of either isoflurane or sevoflurane, consistent with pharmacologically induced bronchoconstriction. Examples of R_L , E_L , and V_D for the same conditions in two representative dogs are shown in Fig. 6. Although R_L and E_L did demonstrate decreases for some dogs during anesthetic delivery (Fig. 6), overall these changes did not result in significant differences for the population. Thus, there were no statistically significant changes for any of the parameters between the maximally constricted state and following delivery of the anesthetic agent. We also did not observe significant differences between targeted and continuous delivery for any of the measurement conditions. Discontinuation of MCh, followed by administration of intravenous atropine, returned R_L , E_L , and V_D to similar levels to their respective baseline values, consistent with reversal of bronchoconstriction.

3.3 Delivered Dose of Anesthetic. Figure 7 shows sevoflurane and isoflurane concentrations, along with corresponding tidal volumes, for two breaths in a representative dog. Data are shown for both targeted and continuous delivery. Compared to continuous delivery, the initial increase in concentration during targeted delivery was delayed until nearly halfway through inspiration, consistent with the delivery threshold, and reached peak concentration at end-inspiration. This delay resulted in considerably lower end-expiration concentrations for targeted delivery, with profiles of isoflurane being similar. By restricting delivery to the end of inspiration, the dogs were exposed to lower doses of inhaled anesthetic for the targeted condition compared to continuous; the average inhaled anesthetic dose per breath following 10 and 20 min of targeted and continuous delivery of sevoflurane and isoflurane are summarized in Fig. 8(a). Doses were similar across animals and were comparable after 10 and 20 min of delivery for a given agent and regimen. Similarly, end-expiratory concentrations were significantly reduced during targeted delivery, while end-inspiratory concentrations were generally similar despite a slightly increased concentration during continuous sevoflurane (Figs. 8(b) and 8(c)).

4 Discussion

In this study, we hypothesized that targeted delivery would promote sufficient anesthetic diffusion directly across the airway wall to reach ASM, resulting in direct relaxation and dilation of constricted airways [20–22]. We used a computer-actuated ventilator-valve circuit to deliver tidal volumes with variable inhaled gas concentrations, and compared estimates of lung resistance, elastance, and anatomic dead space following targeted and continuous delivery of sevoflurane and isoflurane in dogs during cholinergic bronchoconstriction. Our intent was to demonstrate that systemic recirculation of the drug may not be necessary to reduce R_L and E_L . While our data indicate that targeted delivery to the conducting airways lowered systemic absorption of the agent, we were unable to demonstrate that targeted or continuous delivery of inhaled anesthetics at clinically relevant doses were successful at reversing cholinergic bronchoconstriction.

Inhaled anesthetics are potent bronchodilators that promote relaxation of ASM [3–7,13]. Their neutrally-mediated effects are important contributors to bronchodilation [26,27], as clinically

relevant concentrations have been shown to depress bronchoconstriction induced using either nebulized acetylcholine or vagal nerve stimulation [28], while systemic recirculation via the bronchial or pulmonary circulations may also be required for adequate delivery to under-ventilated regions of the lung [36–38]. In addition to these effects, direct diffusion of these agents from lumen to airway wall may be an important mechanism for in vivo bronchodilation. Despite their bronchodilator action, however, we observed that neither targeted nor continuous inhaled anesthetic delivery resulted in significant changes in any of the measured parameters. This is in contrast to previous reports. Ishikawa et al. showed that isoflurane and sevoflurane yielded reductions in R_L and E_L during MCh-induced bronchoconstriction in dogs [39], with estimates of effect size using Cohen's d ranging between 0.6 and 0.8 for isoflurane or sevoflurane at 0.5 or 1.0 MAC. Mitsuhashi et al. showed comparable effects in reversing anaphylaxis in dogs sensitized to *ascaris suum* [40], while other studies have demonstrated comparable protective effects of both inhaled anesthetics in smaller species such as rats and guinea pigs with MCh-induced bronchoconstriction [41,42].

There may be several reasons we were unable to detect significant changes in R_L , E_L , or V_D across our cohort. First, the study ($N=5$) may have been underpowered compared with previous work in which considerably larger animal populations ($N > 20$) were used [39,40]. Although some dogs did demonstrate positive responses to inhaled anesthetic delivery (i.e., reductions in R_L and E_L with increases in V_D), other dogs demonstrated no response at all (Fig. 6). For these nonresponders, continuous MCh infusion may have induced excessive levels of bronchoconstriction that was unresponsive to dilation with inhaled anesthetics. It is possible that these agents are more effective as broncho-protective therapy [40,43] to prevent rather than to reverse cholinergic bronchoconstriction. Alternatively, we may not have achieved sufficient bronchodilation to result in changes in R_L , E_L , and V_D that

were substantial enough to overcome inter- and intrasubject variability in these parameters. It is possible that the total inhaled anesthetic delivered may have been inadequate to achieve equal bronchodilation in each case, either due to insufficient time of administration or delivery concentration. The previously mentioned studies report an increasing dose–response relationship for inhaled anesthetic agents such that larger reductions in R_L and E_L occur for higher MAC. Although we demonstrate similar peak anesthetic concentrations, these increases occur rapidly at the end of inspiration during targeted delivery (Figs. 7(a) and 7(c)), and our ventilator-value configuration produced fluctuations between end-inspiration and end-expiration concentrations within a single breath during continuous delivery (Figs. 7(b) and 7(d)). Thus, the total dose delivered of inhaled anesthetic with the potential to reach and act on the ASM yielding bronchodilation, especially during targeted delivery, would be smaller than that delivered using a standard anesthesia machine at comparable MAC. Finally, the single compartment model used here may oversimplify representations of the heterogeneity induced by the bronchoconstriction and be insensitive to bronchodilatory changes occurring during treatment with inhaled anesthetics as total lung resistance R_L may be more reflective of parenchymal tissue resistance rather than airway resistance [44,45]. Although both may be affected by bronchoconstricting or bronchodilating agonists [46,47], inhaled anesthetic delivery in animal models has been shown to cause airway dilation with little change in the parenchymal mechanics [43,48]. Dynamic lung elastance E_L may also be directly affected by pharmacologic agonism, and be further modulated by airway-tissue interdependence [35]. Therefore, more complex, robust analyses such as forced oscillatory measurements of lung impedance [30,49] coupled with an inverse model topology [31,50,51] may better characterize mechanical heterogeneity compared to the single compartment model by distinguishing between distributed airway or tissue properties.

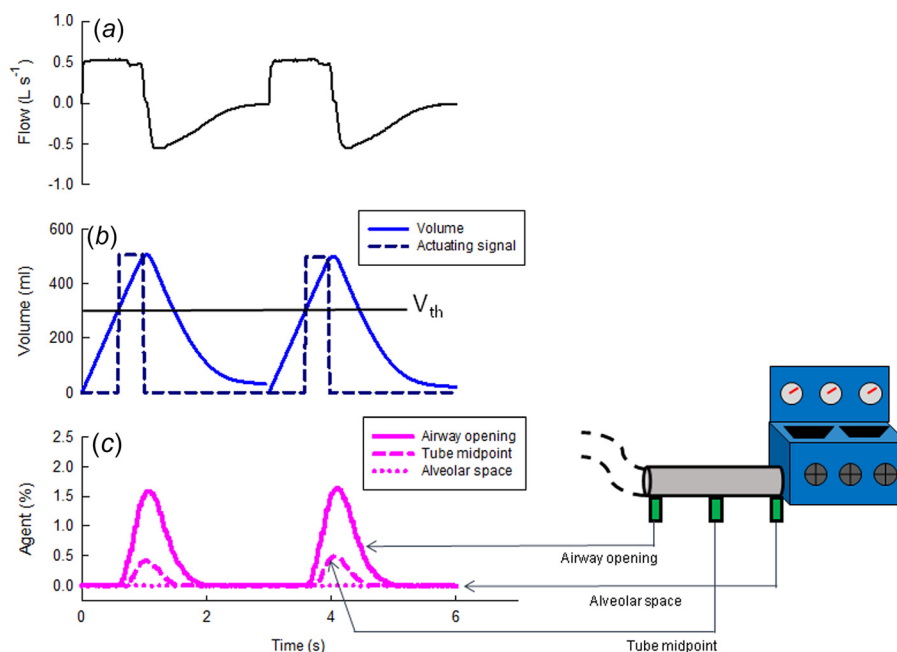


Fig. 4 Isoflurane was delivered to a section of corrugated tubing (~150 ml, gray cylinder) in series with a pair of spring-loaded bellows (as shown on the right in the schematic, ventilated with tidal volume 500 ml and rate 20 min^{-1}): (a) characteristic trace of flow measured for two breaths; (b) corresponding tidal volume (solid) with real-time generation of actuating signal denoting anesthetic delivery window at the end of inspiration (dashed). The delivery threshold (V_{th}) was set to 300 ml to account for the delay in switching between sublimbs and engaging the anesthetic vaporizer; and (c) three traces of isoflurane concentration characterizing anesthetic distribution throughout the dead space compartment. Isoflurane concentration detected at the interface between dead space and alveolar compartments was negligible.

4.1 Ventilation Heterogeneity During Bronchoconstriction. One may further speculate that an uneven distribution of the inhaled anesthetic could have played a critical role in the observed variability between positive and negative responses during bronchoconstriction. Previous modeling studies have shown that asthma is associated with heterogeneous constriction of the airway tree, particularly in *smaller* peripheral airways [52–55], though imaging studies suggest that partial closure of *larger* bronchi also contribute [56–58]. Venegas et al. [59,60] have shown that “bi-stable” terminal airways, which exist as either fully opened or nearly closed, can lead to poorly ventilated lung regions called ventilation defects [50] via dynamic feedback interactions involving both the central bronchi and peripheral airways [59,61].

Consequently, flow redistribution away from such ventilation defects would promote more heterogeneous delivery of the inhaled anesthetic, causing bronchodilation of unaffected airways, which may limit the overall efficacy of these agents, or even potentially increase ventilation heterogeneity. These increases in airway heterogeneity may contribute to substantial increases in apparent R_L and E_L as measured at the airway opening, especially at physiologic breathing frequencies [55], which would potentially mask our ability to detect any bronchodilation resulting from direct action of the inhaled anesthetic on ASM. Similarly, MCh-induced hypersecretion of mucus in the airways [62] may facilitate partial or complete airway closure and formation of mucus plugs [63,64], which would occlude small airways and limit the

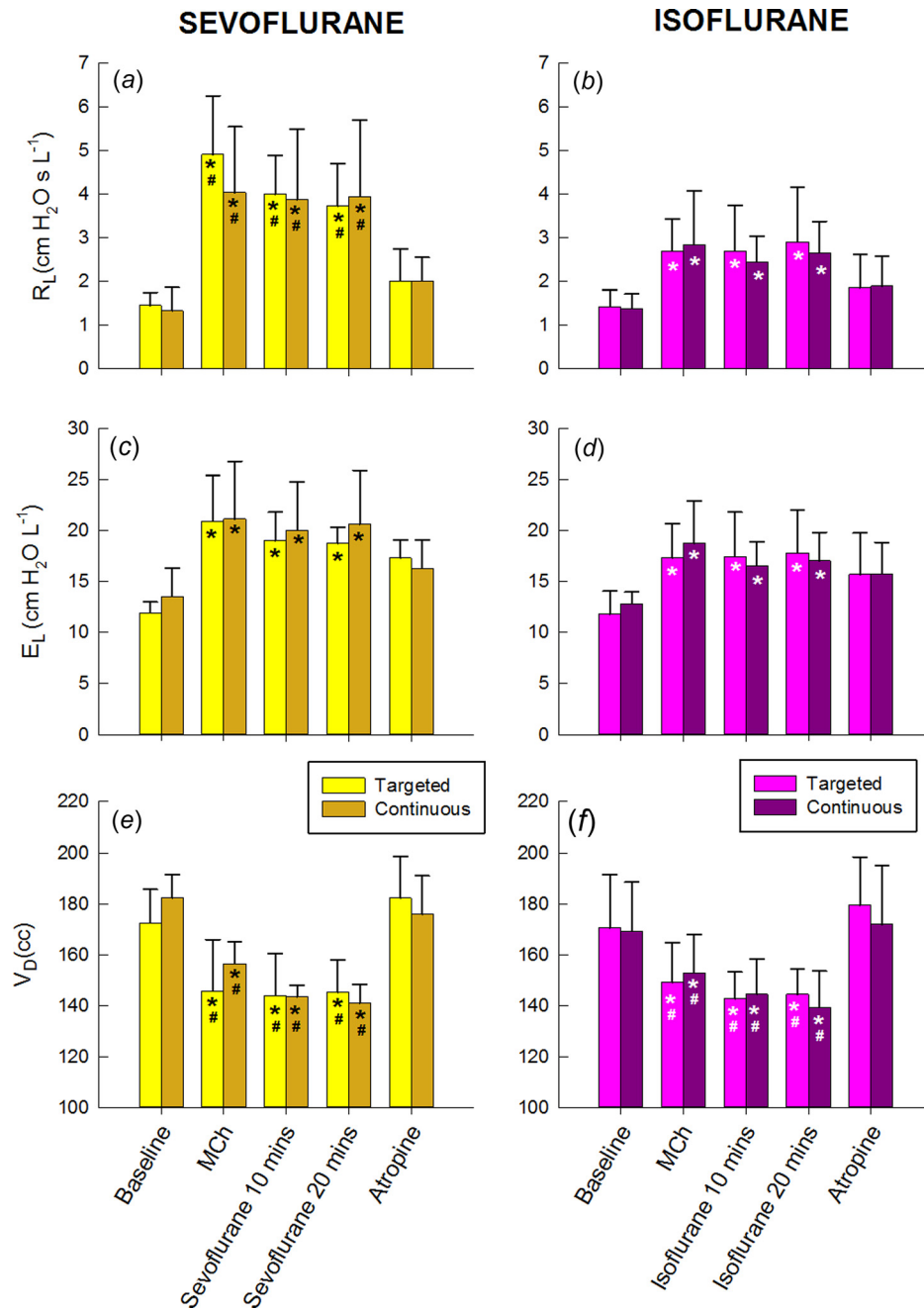


Fig. 5 Summary of: (a) and (b) lung resistance (R_L); (c) and (d) lung elastance (E_L); and (e) and (f) anatomic dead space (V_D) during targeted and continuous delivery. Data are shown for sevoflurane (left panels) and isoflurane (right panels), and are averaged across all animals, with error bars denoting standard deviations. *Significantly different compared to baseline; #significantly different compared to atropine. For all comparisons, $P < 0.05$.

amount of inhaled anesthetic reaching constricted airways. Such an effect would limit the effectiveness of this delivery method and may have played a role in cases where R_L and E_L actually increased and V_D decreased.

4.2 Anesthetic Delivery System. We previously proposed that the serial composition of an inspired gas could be manipulated to target the anatomic dead space [29]. The concept of different portions of the inspired tidal volume having variable gas concentrations is familiar to anesthesiologists using traditional “Mapleson” style semi-open breathing circuits [65]. In a similar study of serial gas manipulation, Brogan et al. [66] demonstrated that ventilation–perfusion matching could be improved by

application of CO_2 to the conducting airways exclusively, with targeted delivery achieved by manual injection of CO_2 during the second half of inspiration. Our anesthetic delivery system advances this method by providing an automated delivery window based on volume capnography, which can be varied to match the subject’s dead space volume. Such a delivery method is not possible with conventional anesthesia machines, which operate via circular breathing circuits designed to maintain a constant agent concentration. While uncommon in general clinical practice, draw-over anesthesia relies on “pulling” fresh gas across a vaporizer during spontaneous breathing of the patient [67]. By combining the U-PAC vaporizer in series with a ventilator, fresh gas can be “pushed” across the vaporizer, facilitating rapid response for

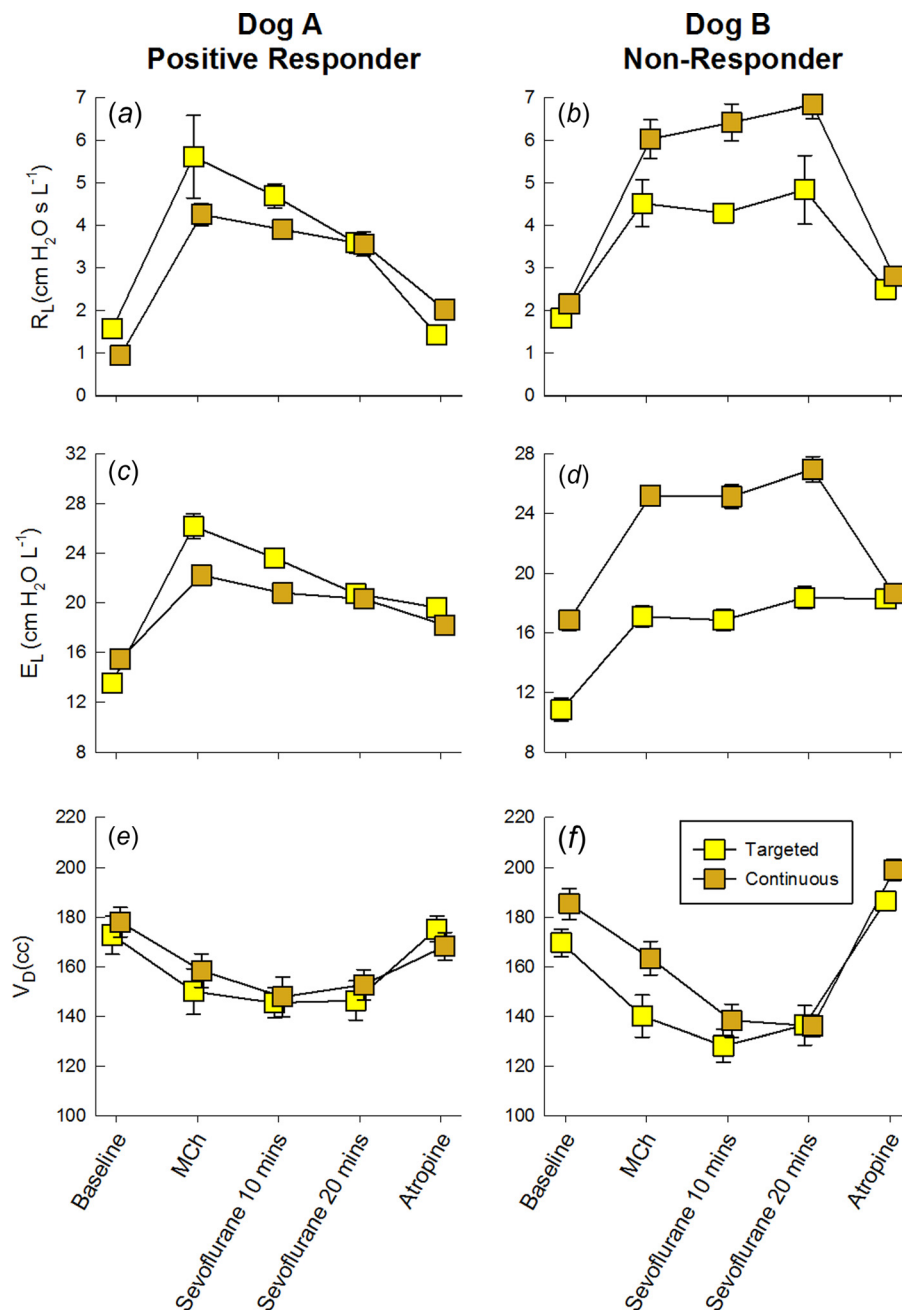


Fig. 6 Examples of (a) and (b) lung resistance (R_L); (c) and (d) lung elastance (E_L); and (e) and (f) anatomic dead space (V_D) during targeted and continuous delivery for two representative dogs. Data are shown for a positive responder (left panels) and a non-responder (right panels) during targeted and continuous sevoflurane delivery. Symbols denote the mean value from 20 breaths. Errors bars, when larger than the symbol, denote standard deviations.

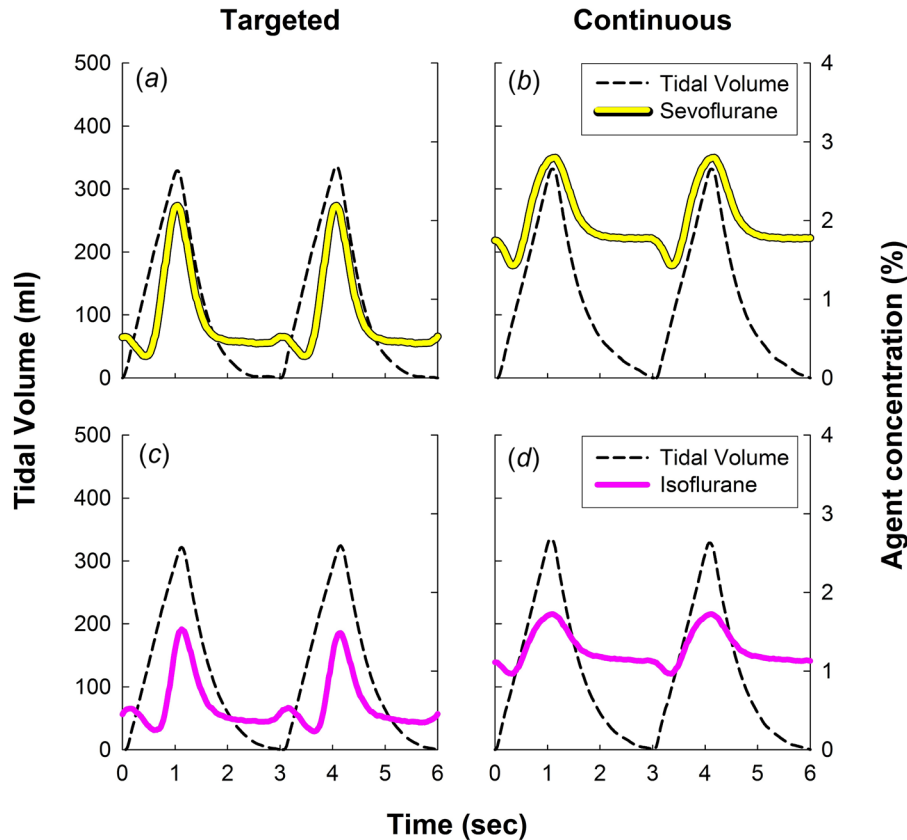


Fig. 7 Example concentration profiles of sevoflurane (solid line) and isoflurane (solid line) measured at the airway opening during (a) and (c) targeted and (b) and (d) continuous delivery, superimposed on corresponding tidal volumes (dashed black line). Note the relatively higher end-expiration concentration for continuous compared to targeted delivery.

targeted delivery of the inhaled anesthetic. The reduced size, compatibility with multiple agents, and operational simplicity of the U-PAC vaporizer provides an ideal method for the delivery of inhaled anesthetics in clinical settings, where there are limited options available for administration of these agents to patients [6].

4.3 Inhaled Anesthetic Exposure. Compared to continuous delivery, we found that targeted delivery resulted in a significantly reduced dose of inhaled anesthetic, as well as a lowered residual concentration at end-expiration (Figs. 7 and 8). This suggests that restricting inhaled anesthetics to the end of inspiration facilitated delivery to the conducting airways while decreasing systemic uptake and redistribution, which is an important consideration given that the consistent clinical use of these agents can be limited by negative systemic side effects [1]. However, a small concentration of end-tidal anesthetic during targeted delivery was still detected (Fig. 8), suggesting that some alveolar delivery and/or uptake of anesthetic via the conducting airways may have occurred [28,37]. Since the canine airway tree is highly asymmetric and leads to a distribution of path lengths between the trachea and terminal alveoli [61], a delivery profile appropriate for longer path lengths would have the potential of anesthetic reaching alveoli at shorter distances relative to the airway opening. While these factors may have resulted in some systemic absorption during targeted delivery, the corresponding end-expiratory concentration was considerably lower compared to that for continuous delivery, consistent with lower systemic absorption of the anesthetics, although not directly measured here.

4.4 Model Critique. Our estimate of anatomic dead space, V_D , is an idealized, compartmentalized physiologic construct

based on capnography, rather than true anatomic measurements of airway size [31]. Increased V_D as an index of bronchodilation may be limited in cases where the lung periphery is the most dominant contributor to increased resistance [35,47], since the conducting airways constitute the majority of anatomic dead space. Yet we observed that changes in V_D and R_L were closely related during maximal bronchoconstriction and airway relaxation with atropine. Therefore, imaging modalities such as high-resolution computed tomographic and magnetic resonance imaging can provide further insight into the ventilation distribution and degree of heterogeneity during bronchoconstriction, while potentially resolving disparities between trends in lung resistance and anatomic dead space [31]. Additionally, these experiments focused on the dilation of constricted airways during cholinergic agonism. Methacholine has been shown to constrict the central airways predominantly, whereas an allergen-induced bronchoconstriction leads to a more peripheral pattern of constriction that can manifest through important ventilation defects as discussed previously [68]. The effects of inhaled anesthetics on this cholinergic pathway may not be similar to their effects on allergic bronchial hyperresponsiveness, for which they are known to be therapeutic [69,70].

5 Conclusions

Despite the known clinical efficacy of inhaled anesthetics for the treatment of severe bronchoconstriction, we did not observe significant *in vivo* bronchodilation following either targeted or continuous delivery of these agents during purely cholinergic bronchoconstriction. Given that this is contrary to previous work, we speculate that higher concentrations delivered to ASM may be necessary to achieve significant bronchodilation using these

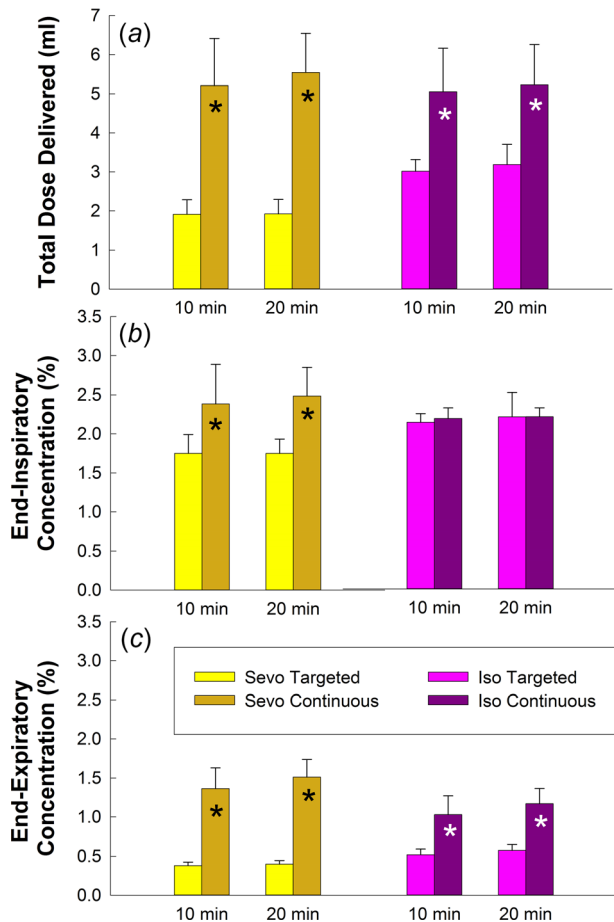


Fig. 8 Comparison of: (a) average inhaled anesthetic dose per breath; (b) end-inspiratory anesthetic concentration; and (c) end-expiratory anesthetic concentration measured during targeted and continuous delivery. Data are shown for sevoflurane (left bars) and isoflurane (right bars). Data are averaged across animals, with error bars denoting SD. *Significantly greater compared to targeted sevoflurane or isoflurane delivery at both 10 and 20 min, $P < 0.05$.

regimens. Protective flow redistribution and hypersecretion of mucus could have limited the amount of inhaled anesthetic delivered to constricted airways, while corresponding increases in lung heterogeneity may have led to increased apparent lung resistance and elastance in some cases. More robust estimates of lung mechanics could help to resolve these discrepancies. Nevertheless, although we were unable to detect significant bronchodilation during inhaled anesthetic delivery, our targeted delivery system indicates that it is possible to deliver inhaled anesthetics predominately to the anatomic dead space, resulting in reduced systemic dose. Thus it may be possible to achieve direct pharmacologic action on airway smooth muscle, with less potential for systemic absorption.

Acknowledgment

The authors gratefully acknowledge General Anesthetic Services, Inc., South Park Township, PA for loan of the U-PAC vaporizer, and Impact Instrumentation, Inc., West Caldwell, NJ for loan of the ventilator. Portions of this work were performed while authors JSM, BAS, and DWK were affiliated with Beth Israel Deaconess Medical Center and Harvard Medical School, Boston, MA, and author JH was affiliated at Boston University, Boston, MA. Authors DWK, JRM, and BAS are listed as inventors on U.S. Patent Application No. US2015/0290418 A1.

Funding Data

- National Heart, Lung, and Blood Institute, Bethesda, MD (HL 089227, HL 108724) and Beth Israel Deaconess Medical Center, Boston, MA.
- National Institute of Biomedical Imaging and Bioengineering, Bethesda, MD (T32 EB006359).

Nomenclature

C_{agent} = anesthetic agent concentration
 E_L = lung elastance
MCh = methacholine
 P_{ao} = airway opening pressure
 P_{es} = esophageal pressure
 P_{tp} = transpulmonary pressure
 P_0 = transpulmonary pressure at end-expiration
 R_L = lung resistance
 V = volume
 \dot{V} = airway opening flow
 V_{agent} = anesthetic agent volume
 V_{alv} = alveolar tidal volume
 V_D = anatomic dead space
 V_T = tidal volume

References

- [1] Tobias, J. D., and Garrett, J. S., 1997, "Therapeutic Options for Severe, Refractory Status Asthmaticus: Inhalational Anaesthetic Agents, Extracorporeal Membrane Oxygenation and Helium/Oxygen Ventilation," *Paediatr. Anaesth.*, **7**(1), pp. 47–57.
- [2] Hebbbar, K. B., Petrillo-Albarano, T., Coto-Puckett, W., Heard, M., Rycus, P. T., and Fortenberry, J. D., 2009, "Experience With Use of Extracorporeal Life Support for Severe Refractory Status Asthmaticus in Children," *Crit. Care*, **13**(2), p. R29.
- [3] Meyer, N. E., and Schotz, S., 1939, "Relief of Severe Intractable Bronchial Asthma With Cyclopropane Anesthesia: Report of a Case," *J. Allergy*, **10**(3), pp. 239–240.
- [4] Schultz, T. E., 2005, "Sevoflurane Administration in Status Asthmaticus: A Case Report," *AANA J.*, **73**(1), pp. 35–36.
- [5] Shankar, V., Churchwell, K. B., and Deshpande, J. K., 2006, "Isoflurane Therapy for Severe Refractory Status Asthmaticus in Children," *Intensive Care Med.*, **32**(6), pp. 927–933.
- [6] Tobias, J. D., 2008, "Therapeutic Applications and Uses of Inhalational Anesthesia in the Pediatric Intensive Care Unit," *Pediatr. Crit. Care Med.*, **9**(2), pp. 169–179.
- [7] Turner, D. A., and Arnold, J. H., 2008, "Improving Our Approach to Sedation in the Pediatric Intensive Care Unit: Is It Time to Inhale?," *Pediatr. Crit. Care Med.*, **9**(2), pp. 233–234.
- [8] Arnold, J. H., Truog, R. D., and Rice, S. A., 1993, "Prolonged Administration of Isoflurane to Pediatric Patients During Mechanical Ventilation," *Anesth. Analg.*, **76**(3), pp. 520–526.
- [9] Best, A., Wenstone, R., and Murphy, P., 1994, "Prolonged Use of Isoflurane in Asthma," *Can. J. Anaesth.*, **41**(5 Pt. 1), pp. 452–453 May.
- [10] Bierman, M. I., Brown, M., Muren, O., Keenan, R. L., and Glauser, F. L., 1986, "Prolonged Isoflurane Anesthesia in Status Asthmaticus," *Crit. Care Med.*, **14**(9), pp. 832–833.
- [11] Miyagi, T., Gushima, Y., Matsumoto, T., Okamoto, K., and Miike, T., 1997, "Prolonged Isoflurane Anesthesia in a Case of Catastrophic Asthma," *Acta Paediatr. Jpn.*, **39**(3), pp. 375–378.
- [12] Mori, N., Nagata, H., Ohta, S., and Suzuki, M., 1996, "Prolonged Sevoflurane Inhalation Was Not Nephrotoxic in Two Patients With Refractory Status Asthmaticus," *Anesth. Analg.*, **83**(1), pp. 189–191.
- [13] Wheeler, D. S., Clapp, C. R., Ponaman, M. L., Bsn, H. M., and Poss, W. B., 2000, "Isoflurane Therapy for Status Asthmaticus in Children: A Case Series and Protocol," *Pediatr. Crit. Care Med.*, **1**(1), pp. 55–59.
- [14] Mazzeo, A. T., Spada, A., Pratico, C., Lucanto, T., and Santamaria, L. B., 2004, "Hypercapnia: What is the Limit in Paediatric Patients? A Case of Near-Fatal Asthma Successfully Treated by Multipharmacological Approach," *Paediatr. Anaesth.*, **14**(7), pp. 596–603.
- [15] Que, J. C., and Lusaya, V. O., 1999, "Sevoflurane Induction for Emergency Cesarean Section in a Parturient in Status Asthmaticus," *Anesthesiology*, **90**(5), pp. 1475–1476.
- [16] Iwaku, F., Otsuka, H., Kuraishi, H., and Suzuki, H., 2005, "The Investigation of Isoflurane Therapy for Status Asthmaticus Patients," *Aerugi*, **54**(1), pp. 18–23.
- [17] O'Rourke, P. P., and Crone, R. K., 1982, "Halothane in Status Asthmaticus," *Crit. Care Med.*, **10**(5), pp. 341–343.
- [18] Burburan, S. M., Xisto, D. G., and Rocco, P. R., 2007, "Anaesthetic Management in Asthma," *Minerva Anesthesiol.*, **73**(6), pp. 357–365.
- [19] Yamakage, M., 2002, "Effects of Anaesthetic Agents on Airway Smooth Muscles," *Br. J. Anaesth.*, **88**(5), pp. 624–627.

- [20] Pabelick, C. M., Prakash, Y. S., Kannan, M. S., Jones, K. A., Warner, D. O., and Sieck, G. C., 1999, "Effect of Halothane on Intracellular Calcium Oscillations in Porcine Tracheal Smooth Muscle Cells," *Am. J. Physiol.*, **276**(1 Pt. 1), pp. L81–L89.
- [21] Yamakage, M., Hirshman, C. A., and Croxton, T. L., 1995, "Volatile Anesthetics Inhibit Voltage-Dependent Ca^{2+} Channels in Porcine Tracheal Smooth Muscle Cells," *Am. J. Physiol.*, **268**(2), pp. L187–L191.
- [22] Yamakage, M., and Namiki, A., 2003, "Cellular Mechanisms of Airway Smooth Muscle Relaxant Effects of Anesthetic Agents," *J. Anesth.*, **17**(4), pp. 251–258.
- [23] Jones, K. A., Wong, G. Y., Lorenz, R. R., Warner, D. O., and Sieck, G. C., 1994, "Effects of Halothane on the Relationship Between Cytosolic Calcium and Force in Airway Smooth Muscle," *Am. J. Physiol.*, **266**(2), pp. L199–L204.
- [24] Schimmel, C., Bernard, S. L., Anderson, J. C., Polissar, N. L., Lakshminarayan, S., and Hlastala, M. P., 2004, "Soluble Gas Exchange in the Pulmonary Airways of Sheep," *J. Appl. Physiol.*, **97**(5), pp. 1702–1708.
- [25] Swenson, E. R., Robertson, H. T., Polissar, N. L., Middaugh, M. E., and Hlastala, M. P., 1992, "Conducting Airway Gas Exchange: Diffusion-Related Differences in Inert Gas Elimination," *J. Appl. Physiol.*, **72**(4), pp. 1581–1588.
- [26] Brown, R. H., Zerhouni, E. A., and Hirshman, C. A., 1993, "Comparison of Low Concentrations of Halothane and Isoflurane as Bronchodilators," *Anesthesiology*, **78**(6), pp. 1097–1101.
- [27] Klide, A. M., and Aviado, D. M., 1967, "Mechanism for the Reduction in Pulmonary Resistance Induced by Halothane," *J. Pharmacol. Exp. Ther.*, **158**(1), pp. 28–35.
- [28] Warner, D. O., Vettermann, J., Brichant, J. F., and Rehder, K., 1990, "Direct and Neurally Mediated Effects of Halothane on Pulmonary Resistance In Vivo," *Anesthesiology*, **72**(6), pp. 1057–1063.
- [29] Mondonedo, J. R., McNeil, J. S., Amin, S. D., Herrmann, J., Simon, B. A., and Kaczka, D. W., 2014, "Volatile Anesthetics and the Treatment of Severe Bronchoconstriction: A Concept of Targeted Delivery," *Drug Discovery Today: Disease Models*, **15**, pp. 43–50.
- [30] Kaczka, D. W., Barnas, G. M., Suki, B., and Lutchen, K. R., 1995, "Assessment of Time-Domain Analyses for Estimation of Low-Frequency Respiratory Mechanical Properties and Impedance Spectra," *Ann. Biomed. Eng.*, **23**(2), pp. 135–151.
- [31] Kaczka, D. W., Brown, R. H., and Mitzner, W., 2009, "Assessment of Heterogeneous Airway Constriction in Dogs: A Structure-Function Analysis," *J. Appl. Physiol.*, **106**(2), pp. 520–530.
- [32] Kazama, T., and Ikeda, K., 1988, "Comparison of MAC and the Rate of Rise of Alveolar Concentration of Sevoflurane With Halothane and Isoflurane in the Dog," *Anesthesiology*, **68**(3), pp. 435–437.
- [33] Lorino, A. M., Beydon, L., Mariette, C., Dahan, E., and Lorino, H., 1996, "A New Correction Technique for Measuring Respiratory Impedance Through an Endotracheal Tube," *Eur. Respir. J.*, **9**(5), pp. 1079–1086.
- [34] Fletcher, R., Jonson, B., Cumming, G., and Brew, J., 1981, "The Concept of DeadSpace With Special Reference to the Single Breath Test for Carbon Dioxide," *Br. J. Anaesth.*, **53**(1), pp. 77–88.
- [35] Kaczka, D. W., Mitzner, W., and Brown, R. H., 2013, "Effects of Lung Inflation on Airway Heterogeneity During Histaminergic Bronchoconstriction," *J. Appl. Physiol.*, **115**(5), pp. 626–633.
- [36] Butler, J., 1991, "The Bronchial Circulation," *News Physiol. Sci.*, **6**(1), pp. 21–25.
- [37] Kelly, L., Kolbe, J., Mitzner, W., Spannake, E. W., Bromberger-Barnea, B., and Menkes, H., 1986, "Bronchial Blood Flow Affects Recovery From Constriction in Dog Lung Periphery," *J. Appl. Physiol.*, **60**(6), pp. 1954–1959.
- [38] Labiris, N. R., and Dolovich, M. B., 2003, "Pulmonary Drug Delivery—Part I: Physiological Factors Affecting Therapeutic Effectiveness of Aerosolized Medications," *Br. J. Clin. Pharmacol.*, **56**(6), pp. 588–599.
- [39] Ishikawa, T., Shinozuka, N., Sato, J., and Nishino, T., 1998, "Inhalation Anaesthetics Produce Asynchronous Reversal of Ventilation Inhomogeneity and Increased Lung Resistance in a Canine Model of Bronchial Asthma," *Br. J. Anaesth.*, **80**(6), pp. 807–813.
- [40] Mitsuhashi, H., Saitoh, J., Shimizu, R., Takeuchi, H., Hasome, N., and Horiguchi, Y., 1994, "Sevoflurane and Isoflurane Protect Against Bronchospasm in Dogs," *Anesthesiology*, **81**(5), pp. 1230–1234.
- [41] Habre, W., Peták, F., Sly, P. D., Hantos, Z., and Morel, D. R., 2001, "Protective Effects of Volatile Agents Against Methacholine-Induced Bronchoconstriction in Rats," *Anesthesiology*, **94**(2), pp. 348–353.
- [42] Schutz, N., Petak, F., Barazzzone-Argiroffo, C., Fontao, F., and Habre, W., 2004, "Effects of Volatile Anaesthetic Agents on Enhanced Airway Tone in Sensitized guinea Pigs," *Br. J. Anaesth.*, **92**(2), pp. 254–260.
- [43] Myers, C. F., Fontao, F., János, T. Z., Boda, K., Peták, F., and Habre, W., 2011, "Sevoflurane and Desflurane Protect Cholinergic-Induced Bronchoconstriction of Hyperreactive Airways in Rabbits," *Can. J. Anaesth.*, **58**(11), pp. 1007–1015.
- [44] Kaczka, D. W., and Smallwood, J. L., 2012, "Constant-Phase Descriptions of Canine Lung, Chest Wall, and Total Respiratory System Viscoelasticity: Effects of Distending Pressure," *Respir. Physiol. Neurobiol.*, **183**(2), pp. 75–84.
- [45] Warner, D. O., Vettermann, J., Brusasco, V., and Rehder, K., 1989, "Pulmonary Resistance During Halothane Anesthesia Is Not Determined Only by Airway Caliber," *Anesthesiology*, **70**(3), pp. 453–460.
- [46] Fredberg, J. J., Bunk, D., Ingenito, E., and Shore, S. A., 1993, "Tissue Resistance and the Contractile State of Lung Parenchyma," *J. Appl. Physiol.*, **74**(3), pp. 1387–1397.
- [47] Kaczka, D. W., Ingenito, E. P., Israel, E., and Lutchen, K. R., 1999, "Airway and Lung Tissue Mechanics in Asthma. Effects of Albuterol," *Am. J. Respir. Crit. Care Med.*, **159**(1), pp. 169–178.
- [48] Sato, J., Shinozuka, N., Kochi, A., Uchida, H., and Mizuguchi, T., 1995, "Low-Dose Halothane Produces Airway Dilatation but Does Not Alter Parenchymal Mechanics in the Normal Canine Lung," *Can. J. Anaesth.*, **42**(5), pp. 438–445.
- [49] Kaczka, D. W., and Dellaca, R. L., 2011, "Oscillation Mechanics of the Respiratory System: Applications to Lung Disease," *Crit. Rev. Biomed. Eng.*, **39**(4), pp. 337–359.
- [50] Kaczka, D. W., Lutchen, K. R., and Hantos, Z., 2011, "Emergent Behavior of Regional Heterogeneity in the Lung and Its Effects on Respiratory Impedance," *J. Appl. Physiol.*, **110**(5), pp. 1473–1481.
- [51] Kaczka, D. W., Massa, C. B., and Simon, B. A., 2007, "Reliability of Estimating Stochastic Lung Tissue Heterogeneity From Pulmonary Impedance Spectra: A Forward-Inverse Modeling Study," *Ann. Biomed. Eng.*, **35**(10), pp. 1722–1738.
- [52] Gillis, H. L., and Lutchen, K. R., 1999, "How Heterogeneous Bronchoconstriction Affects Ventilation Distribution in Human Lungs: A Morphometric Model," *Ann. Biomed. Eng.*, **27**(3), pp. 14–22.
- [53] Gillis, H. L., and Lutchen, K. R., 1999, "Airway Remodeling in Asthma Amplifies Heterogeneities in Smooth Muscle Shortening Causing Hyperresponsiveness," *J. Appl. Physiol.*, **86**(6), pp. 2001–2012.
- [54] Lutchen, K. R., and Gillis, H., 1997, "Relationship Between Heterogeneous Changes in Airway Morphometry and Lung Resistance and Elastance," *J. Appl. Physiol.*, **83**(4), pp. 1192–1201.
- [55] Lutchen, K. R., Greenstein, J. L., and Suki, B., 1996, "How Inhomogeneities and Airway Walls Affect Frequency Dependence and Separation of Airway and Tissue Properties," *J. Appl. Physiol.*, **80**(5), pp. 1696–1707.
- [56] Tzeng, Y. S., Hoffman, E., Cook-Granroth, J., Gereige, J., Mansour, J., Washko, G., Cho, M., Stepp, E., Lutchen, K., and Albert, M., 2008, "Investigation of Hyperpolarized ^3He Magnetic Resonance Imaging Utility in Examining Human Airway Diameter Behavior in Asthma Through Comparison With High-Resolution Computed Tomography," *Acad. Radiol.*, **15**(6), pp. 799–808.
- [57] Tzeng, Y. S., Lutchen, K., and Albert, M., 2009, "The Difference in Ventilation Heterogeneity Between Asthmatic and Healthy Subjects Quantified Using Hyperpolarized ^3He MRI," *J. Appl. Physiol.*, **106**(3), pp. 813–822.
- [58] Venegas, J. G., Schroeder, T., Harris, S., Winkler, R. T., and Melo, M. F., 2005, "The Distribution of Ventilation During Bronchoconstriction is Patchy and Bimodal: A PET Imaging Study," *Respir. Physiol. Neurobiol.*, **148**(1–2), pp. 57–64.
- [59] Venegas, J. G., Winkler, T., Musch, G., Vidal Melo, M. F., Layfield, D., Tgavalekos, N., Fischman, A. J., Callahan, R. J., Bellani, G., and Harris, R. S., 2005, "Self-Organized Patchiness in Asthma as a Prelude to Catastrophic Shifts," *Nature*, **434**(7034), pp. 777–782.
- [60] Winkler, T., and Venegas, J. G., 2007, "Complex Airway Behavior and Paradoxical Responses to Bronchoprovocation," *J. Appl. Physiol.*, **103**(2), pp. 655–663.
- [61] Amini, R., and Kaczka, D. W., 2013, "Impact of Ventilation Frequency and Parenchymal Stiffness on Flow and Pressure Distribution in a Canine Lung Model," *Ann. Biomed. Eng.*, **41**(12), pp. 2699–2711.
- [62] Rubin, B. K., Priftis, K. N., Schmidt, H. J., and Henke, M. O., 2014, "Secretory Hyperresponsiveness and Pulmonary Mucus Hypersecretion," *Chest*, **146**(2), pp. 496–507.
- [63] Yager, D., Kamm, R. D., and Drazen, J. M., 1995, "Airway Wall Liquid. Sources and Role as an Amplifier of Bronchoconstriction," *Chest*, **107**(3), pp. 105S–110S.
- [64] Hill, M. J., Wilson, T. A., and Lambert, R. K., 1997, "Effects of Surface Tension and Intraluminal Fluid on Mechanics of Small Airways," *J. Appl. Physiol.*, **82**(1), pp. 233–239.
- [65] Lovich, M. A., Simon, B. A., Venegas, J. G., Sims, N. M., and Cooper, J. B., 1993, "A Mass Balance Model for the Mapleson D Anaesthesia Breathing System," *Can. J. Anaesth.*, **40**(6), pp. 554–567.
- [66] Brogan, T. V., Robertson, H. T., Lamm, W. J., Souders, J. E., and Swenson, E. R., 2004, "Carbon Dioxide Added Late in Inspiration Reduces Ventilation-Perfusion Heterogeneity Without Causing Respiratory Acidosis," *J. Appl. Physiol.*, **96**(5), pp. 1894–1898.
- [67] Gegel, B. T., 2008, "A Field-Expedient Ohmeda Universal Portable Anesthesia Complete Draw-Over Vaporizer Setup," *AANA J.*, **76**(3), pp. 185–187.
- [68] Bayat, S., Strengell, S., Porra, L., Janosi, T. Z., Petak, F., Suhonen, H., Suortti, P., Hantos, Z., Sovijärvi, A. R., and Habre, W., 2009, "Methacholine and Ovalbumin Challenges Assessed by Forced Oscillations and Synchrotron Lung Imaging," *Am. J. Respir. Crit. Care Med.*, **180**(4), pp. 296–303.
- [69] Burburan, S. M., Silva, J. D., Abreu, S. C., Samary, C. S., Guimaraes, I. H., Xisto, D. G., Morales, M. M., and Rocco, P. R., 2014, "Effects of Inhalational Anaesthetics in Experimental Allergic Asthma," *Anaesthesia*, **69**(6), pp. 573–582.
- [70] Burburan, S. M., Xisto, D. G., Ferreira, H. C., Riva Ddos, R., Carvalho, G. M., Zin, W. A., and Rocco, P. R., 2007, "Lung Mechanics and Histology During Sevoflurane Anesthesia in a Model of Chronic Allergic Asthma," *Anesth. Analg.*, **104**(3), pp. 631–637.